



CHORUS

This is the accepted manuscript made available via CHORUS. The article has been published as:

Photothermal Response in Dual-Gated Bilayer Graphene

M.-H. Kim, J. Yan, R. J. Suess, T. E. Murphy, M. S. Fuhrer, and H. D. Drew

Phys. Rev. Lett. **110**, 247402 — Published 14 June 2013

DOI: [10.1103/PhysRevLett.110.247402](https://doi.org/10.1103/PhysRevLett.110.247402)

Photo-thermal response in dual-gated bilayer graphene

M.-H. Kim,¹ J. Yan,^{1,2} R. J. Suess,³ T. E. Murphy,³ M. S. Fuhrer,¹ and H. D. Drew¹

¹*Center for Nanophysics and Advanced Materials, Department of Physics,
University of Maryland, College Park, Maryland 20742, USA*

²*Physics Department, University of Massachusetts, Amherst, MA 01002, USA*

³*Institute for Research in Electronics and Applied Physics,
University of Maryland, College Park, Maryland 20742, USA*

The photovoltaic and bolometric photoresponse in gapped bilayer graphene was investigated by optical and transport measurements. A pulse coincidence technique at $1.5\ \mu\text{m}$ was used to measure the response times as a function of temperature. The bolometric and photovoltaic response times were found to be identical implying that the photovoltaic response is also governed by hot electron thermal relaxation. Response times of $\tau \sim 100 - 20\ \text{ps}$ were found for temperatures from 3 - 100 K. Above 10 K, the relaxation time was observed to be $\tau = 25 \pm 5\ \text{ps}$, independent of temperature within noise.

PACS numbers: 78.67.Wj, 78.47.D-, 78.56.-a

There is growing recognition that graphene has exceptional potential as a new optoelectronic material, which has led to a flurry of recent research activity and rapid advances. [1–3] Graphene’s unique massless band structure gives rise to direct transitions and strong (specific) coupling to light at all wavelengths, [4] ultra-fast response (from nanosecond to femtosecond) [4] room temperature operation for many applications. A photovoltaic response has been observed for visible light and we have recently observed both photovoltaic and bolometric response in bilayer graphene at THz frequencies. [5] Diode-like rectification behavior is observed with contacts to dissimilar metals. [1, 2, 5, 6] However, the mechanism of the photovoltaic response has not been definitively identified. Both p-n junction physics similar to conventional semiconductor photovoltaic sensors and a thermoelectric mechanism remain viable possibilities. A photoconductive response was recently reported in biased graphene. [7] In a recent study we observed a hot electron bolometric response in gapped bilayer graphene, which highlighted the outstanding thermal properties of graphene. [5] Therefore, understanding the role of hot electron effects in the photoresponse of graphene may be key to the development of graphene-based optoelectronic devices such as bolometers and photovoltaic sensors. [8]

Excited electrons in graphene thermalize quickly on the femtosecond time scales [9, 10] by electron-electron scattering. [11] These hot electrons transfer their thermal energy to the graphene lattice by the emission of phonons on a much longer time scale because of the weak electron-phonon interaction. [11–14] The thermal relaxation of hot electrons by optical phonons in graphene or in the substrate [10, 15–19] and by acoustic phonons [5, 20] has received much recent attention. The optical phonon cooling occurs on the ps time scale. Acoustic phonon assisted cooling with ns to sub-nanosecond timescales is dominant for longer times and/or lower temperatures or pulse radiation energy. [5, 17, 20]

Hot electrons can be utilized for bolometric and photovoltaic photoresponse detection. [5, 8, 21] The bolometric response makes use of the temperature dependence of the resistivity, which is significant in gapped bilayer graphene. On the other hand, the hot electrons can also give rise to a photo-thermoelectric response. Diffusion of heat and carriers to the contacts produce a thermoelectric response. A competing mechanism for photovoltaic response is charge separation by the built-in electric fields at metal-graphene junctions due to proximity doping. [1, 2] Delineating the relative importance of these two mechanisms in graphene photovoltaic devices is an important topic in graphene photodetector research.

In this paper, we use electrical transport and optical photoresponse measurements to characterize the bolometric and photovoltaic response of a dual-gated bilayer graphene device. The temperature-dependent resistance of the device allows a bolometric response which is characterized both optically and with AC transport measurements. [5] We find that light also generates a voltage across the sample with zero bias current. We compare this photovoltaic response with the well characterized bolometric signal in the same device as functions of dual-gate voltages and temperature. In particular pulse coincidence measurements reveal that the photo voltage has the same temperature and gate-dependent relaxation time as the bolometric response, demonstrating that diffusive hot carrier relaxation in graphene underlies the observed photo voltage of the device.

The bilayer graphene device we studied was fabricated by mechanical exfoliation of natural graphite on a resistive silicon wafer ($200\ \Omega\text{cm}$) which was ion implanted with boron to provide a highly conducting but transparent back-gate. A 300 nm thick SiO_2 layer was then grown by dry oxidation on the silicon wafer. A micrograph of the device is shown in Fig. 1(a) inset and a schematic device geometry is shown in Fig. 1(b) inset. A thin Nichrome film was used as a semitransparent top-gate.

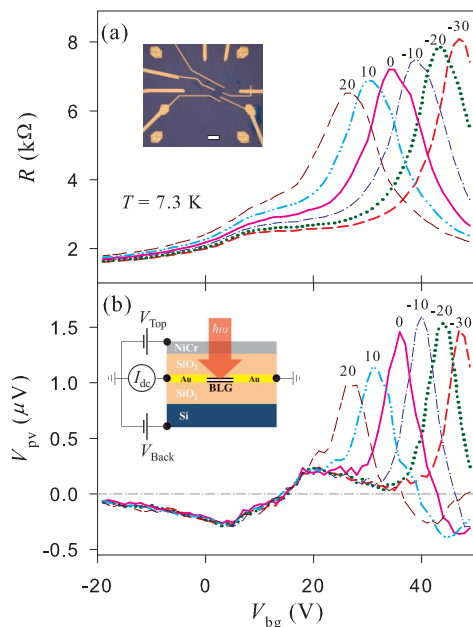


FIG. 1. **Photovoltaic response and resistance of a dual-gated bilayer graphene.** (a) Resistance and (b) photovoltaic response as a function of back gate voltage for different top gate voltages at $T = 7.3$ K and zero bias current. Inset in (a) shows an optical micrograph of the bilayer graphene device. Scale bar, $10\mu\text{m}$. Inset in (b) shows schematic of device geometry and electric-field-effect gating.

Details of the device structure and the gating scheme can be found in Ref. 5. The dual-gated structure allows for independent tuning of carrier density and bandgap of the bilayer graphene device. In this work we gated the device for a small band gap which diminishes the bolometric response making the photovoltaic response more evident. Figure 1(a) shows the device resistance R at 7.3 K as a function of back gate voltage V_{bg} at various top gate voltages V_{tg} . A broad resistance peak appears near $V_{bg} = 10$ V independent of V_{tg} and is attributed to the part of the bilayer device that is not gated by the top gate. [22] The other sharper peak shifts with V_{tg} and is attributed to the charge neutral point of the dual-gated region of the device.

At low temperatures and moderate bias currents the photoresponse is dominated by the bolometric response. Due to disorder the resistance has a power law dependence ($R \sim T^{-0.06}$), which is weaker than the dependence reported earlier for a device with a larger band gap. [5] The photovoltaic response V_{pv} shown in Fig. 1(b) was measured with bias current $I_{dc} = 0$. Near $V_{bg} = 10$ V where R has a broad peak V_{pv} doesn't depend on V_{tg} , and V_{pv} crosses zero at $V_{bg} \approx 15$ V. This behavior is similar to that observed in photo-thermoelectric results reported in graphene. [8, 16, 23] For $V_{bg} > 20$ V, V_{pv} depends on both V_{tg} and V_{bg} , and reaches its maximum at the maximum R . The photo-thermoelectric response re-

quires some asymmetry in the sample, such as contacts with dissimilar metal or size, non-uniform heating, or inhomogeneous doping. The asymmetries in our device are inadvertent and the thermal voltages are much smaller than expected for a device optimized for photothermal response. We note that the bias voltages used for our bolometric signals were in the mV range, much smaller than the gate voltages and too small for significant photocurrent generation as reported by Freitag et. al. [7]

To measure the response times of these signals we used a pulse coincidence technique. The photoresponse was studied at $1.56\mu\text{m}$ with a pulsed laser with a 65-fs pulse width and 100 MHz repetition rate. Pulses from two fiber lasers (Menlo Systems) are locked together with a tunable time separation at repetition rate near 100 MHz, which allows pulse coincidence measurements with precise time delays from a few ps to 10 ns without a mechanical delay line. To avoid parasitics the optical signals are then chopped at 1 kHz and the average photovoltage is measured with a lock-in amplifier. The absorption of $1.56\mu\text{m}$ radiation in the graphene was estimated to be 1.2% by considering effects due to the silicon substrate and the Nichrome top gate. [5] The graphene absorbs an average power of 0.37 nW from the pump and probe pulses and generates a temperature rise ΔT . From the estimated heat capacity of the graphene (discussed later) we estimate the peak ΔT to be 10 K at $T_0 = 10$ K and 0.5 K at room temperature. We also note that at the low laser pulse energies of these experiments the carrier densities are not changed significantly.

The dependence of the photoresponse with pulse time delay for different bias currents is shown in Fig. 2(a) under conditions that the device is gated to its charge neutral point. We find that the total photoresponse can be described as $V_{pr}(I_{dc}) = V_b(I_{dc}) + V_{pv}$ allowing a separation of the photovoltaic and bolometric contributions. The bolometric signal given by $V_b = I_{dc}\Delta R$ was reported earlier. [5] It is seen in the figure that this bolometric response is dominant except near $I_{dc} = 0$ where the response is purely photovoltaic.

These pulse time delay data allow a measurement of the response time τ of the two components of the photoresponse. For long pulse delay times, t_d , average probe-pulse induced photo voltage, V_{pr} is independent of t_d . When the delay is short ($t_d < \tau$), however, the magnitude of V_{pr} is reduced due to the nonlinear radiation power dependence of the response so that the photo voltage $V_{pr}(t_d)$ displays a peak or dip at $t_d = 0$. The magnitude of this peak or dip increases with the non-linear power dependence of V_{pr} .

Figure 2(b) shows V_{pv} and $V_b(I_{dc})$ normalized to the response at longer time delay for several different I_{dc} . All of the normalized V_b for different I_{dc} collapse to one curve because the small Joule heating $I_{dc}^2 R$ does not significantly raise the electron temperature. Surprisingly, the widths of both bolometric and photovoltaic dips near

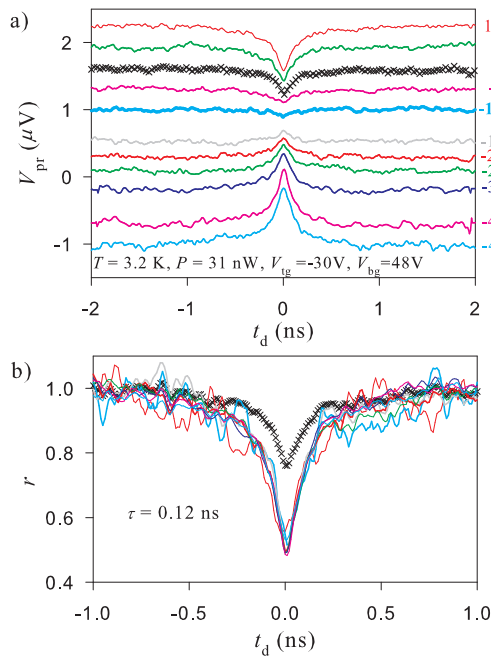


FIG. 2. **Bias current dependence of the pump-probe measurements.** Photoresponse from pump-probe laser pulses as a function of time delay t_d at 3.2 K and laser power of 31 nW. The sample is gated to charge neutrality with $V_{tg} = -30$ V, $V_{bg} = 48$ V. (a) Bias current I_{dc} dependence of probe-induced photoresponse voltage $V_{pr}(t_d)$ as a function of the probe beam delay time t_d . The $I_{dc} = 0$ curve is the photovoltaic response. (b) r is the normalized bolometric response $\Delta V(I_{dc}) = V(I_{dc}) - V(0)$ and photovoltaic response $V(0)$. $r = V_{pr}(t_d)/V_{pv}^0$, where $V_{pv}^0 = V_{pv}(t_d \gg \tau)$. The thermal response time τ is defined as the half-width at half-maximum of the dip. All dips have a similar time constant $\tau = 0.12 \pm 0.01$ ns.

zero time delay are seen to be the same to within the experimental error. The time constants determined by the half widths at half maximum of the dips are 0.12 ± 0.01 ns. This demonstrates that both V_{pv} and $V_b(I_{dc})$ have the same response times. Similar results are observed at different gating conditions and temperatures. Since the bolometric response is clearly thermal as was demonstrated earlier, [5] these data imply that the photovoltaic response is also thermal in nature.

To gain further insight into the nature of the photovoltaic response, we measured its gate voltage dependence. Figure 3 shows back gate voltage dependence of photo voltage at $T = 15$ K with $V_{tg} = 0$ and $I_{dc} = 0$. As can be seen from the data in Fig. 1(a), the top gate does not gate the entire device. To obtain uniform gating we control only the back gate voltage with zero top gate voltage. Figures 3(a) and (b) display the photovoltaic response below and above the maximum V_{pv} observed at around $V_{bg} = 25$ V. The peak or dip structure is associated with the sign of V_{pv} , and its depth or height depends on the nonlinear power dependence of

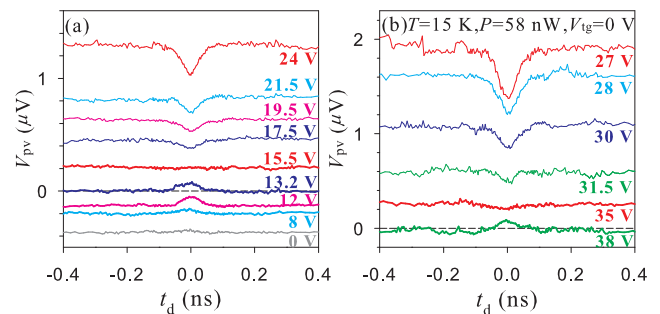


FIG. 3. **Gate voltage dependence of the pump-probe measurements.** Pump-probe pulse induced photovoltaic response as a function of time delay at 15 K and laser power of 58 nW. $I_{dc} = 0$. The data was taken at several back gate voltages V_{bg} with zero top gate voltage (a) below and (b) above $V_{bg} = 25$ V where the maximum photovoltaic response is found. The thin dashed line at $V_{bg} = 0$ is a guide line. All cusps have the same thermal time constant $\tau = 25 \pm 5$ ps within error.

V_{pv} . Both sign and power nonlinearity depend on back gate voltage. For example, at $V_{bg} = 15.5$ V the response $V_{pv}(t_d)$ is independent of t_d indicating that V_{pv} is linear with radiation power. As the power nonlinearity of V_{pv} grows above or below $V_{bg} = 15.5$ V, the dip or peak of V_{pv} appears and grows. Remarkably, however, all of the pump-probe data have the same $\tau = 25$ ps ± 5 ps. The gate-independent time constant shows that the photovoltaic response is thermal at all gate voltages not only at maximum R with respect to V_{bg} as shown in Fig. 2(b) where it could be directly compared with the bolometric response. This observation demonstrates that the photovoltaic response time in bilayer graphene does not depend significantly on gating conditions.

Figure 4 exhibits the temperature dependence of the photoresponse time obtained from the pulse coincidence technique in the temperature range 3 K - 87 K and at several different dual-gate voltages. Again, the response time for different gate voltages are seen to coincide within error. The time constant is found to decrease from ~ 80 ps at 3 K to ~ 20 ps at 80 K. Above $T \sim 10$ K, τ is seen to be nearly temperature independent to within experimental error.

The thermal relaxation rate due to acoustic phonon emission is given by the ratio of the electronic heat capacity C to thermal conductance G . The thermal conductance was obtained using transport measurements as described in Ref. 5. Optical phonons for graphene and the substrate can also provide cooling of the electrons [17]. Although we cannot rule these processes out, they are activated we expect them to be suppressed far below the acoustic phonon effects at the temperature of our experiments. For $T < 8$ K, the transport measurements gives $G = 0.5 \times (T/5)^{3.45}$ nW/K which is in reasonable agreement with the value estimated for cooling by

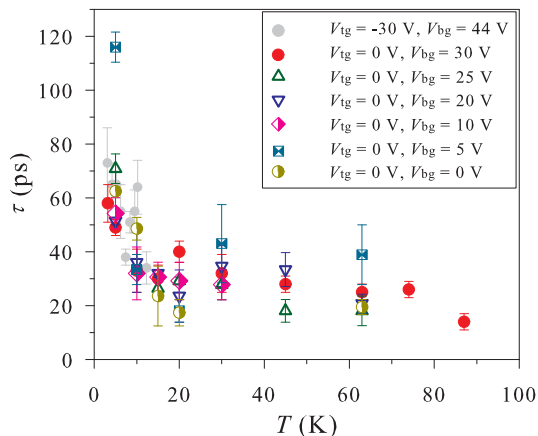


FIG. 4. **Temperature dependence of thermal response time.** Thermal time constant τ of the photovoltaic response vs. temperature measured by the pulse coincidence technique for several different dual-gate voltage settings.

acoustic phonons. [14] A crossover of the thermal conductance from T^3 to linear T is predicted at $T \approx T_{BG}$, where T_{BG} is the Bloch-Grünheisen temperature given by $k_B T_{BG} \approx 2\hbar v_s k_F$. [14] Assuming a sound velocity $v_s = 2.6 \times 10^4$ m/s [24] and a disorder-induced charge density of $n_{rms} \sim 10^{12}$ cm $^{-2}$ [25], we estimate $T_{BG} \sim 70$ K. Although our sample is nominally charge neutral at R_{max} , it is widely accepted that disorder creates electron-hole puddles [26] and thus the effective T_{BG} is non-zero at all gate voltages. Transport measurements show that the Bloch-Grünheisen regime behavior occurs for $T < 0.2T_{BG} \sim 14$ K. [24] The behavior of G and C above $T \sim 0.2T_{BG}$ may be complicated by disorder induced supercollision cooling [20, 27] and/or the non-parabolic band structure of gapped bilayer graphene [4] which leads to small Fermi energies. We measured $G = 0.91 \times T^{1.04}$ nW/K for $T > 8$ K, which is reasonable in view of these considerations.

On the other hand, diffusion cooling of hot electrons also produces a nearly linear T dependent thermal conductance. Diffusion cooling provides a thermal conductance $k = \Lambda T/R_g$, by the Wiedermann-Franz law, where $\Lambda = \pi^2 k_B^2/3e^2$ is the Lorentz number, and R_g is the resistance. At the peak resistance for our sample, $k = 3.4 \times 10^{-12} \times T^{1.0}$ W/K, which is two orders of magnitude smaller than the electron-phonon conductance. We conclude that acoustic phonon mediated cooling of hot electrons is dominant in our devices.

We note, however, that the thermoelectric and photo thermovoltic signals are a consequence of diffusion. For asymmetric contacts the thermal diffusion and charge flow at the two contacts differs leading to a net potential difference. The diffusion length $\xi = (k/G)^{1/2}$ is estimated to be $0.5 \mu\text{m}$ at 10 K which is much smaller than the sample size of $5 \mu\text{m}$ so that the sample temperature rise and response time is dominated by the thermal con-

ductance to the lattice which greatly reduces the thermoelectric signals in these large area, low conductance samples.

At low temperatures ($k_B T < \mu$, where μ is the local Fermi energy in the graphene and k_B is the Boltzmann constant) the electronic specific heat is $C = \alpha T$, where $\alpha = (\pi^2/3)v(E_F)k_B^2$, where $v(E_F)$ is the density of states for bilayer graphene. In the parabolic band approximation of (ungapped) graphene $v(E_F) \approx \gamma_1/(\pi\hbar^2 v_F^2)$ where the interlayer coupling $\gamma_1 = 390$ meV [28], $v_F = 1 \times 10^6$ m/s is the monolayer graphene Fermi velocity. For our sample area of $25 \mu\text{m}^2$, this gives $\alpha = 2.6 \times 10^{-20}$ J/K 2 . Thus the thermal response time of our bilayer sample can be estimated $\tau = C/G \approx 29$ ps independent of temperature for $T > 8$ K which is in reasonable agreement with the measured τ shown in Fig. 4.

In summary, we have reported photovoltaic response time measurements on gapped bilayer graphene. The devices show both bolometric and photovoltaic responses, which were separated by their bias current dependence. The identical response time constants observed for the bolometric and photovoltaic responses as a function of gate voltages and temperature implies that both effects are governed by the same intrinsic hot electron-phonon thermal relaxation process. The observed response times of 10 - 100 ps indicates that hot electron relaxation occurs through acoustic phonon emission. These observations support the growing realization that graphene has great promise for fast sensitive photo detectors over a wide spectral range and they highlight the hot carrier nature of the optical response.

The authors thank A. B. Sushkov, G. S. Jenkins, and D. C. Schmadel for helping with the optical cryostat setup and for valuable discussions. This work was supported by IARPA, the ONR MURI program and the NSF (grants DMR-0804976 and DMR-1105224) and in part by the NSF MRSEC (grant DMR-0520471).

-
- [1] F. Xia, T. Mueller, Y.-M. Lin, A. Valdes-Garcia, and P. Avouris, *Nature Nanotech.* **4**, 839 (2009).
- [2] T. Mueller, F. Xia, and P. Avouris, *Nature Photonics* **4**, 297 (2010).
- [3] T. J. Echtermeyer, L. Britnell, P. K. Jasnós, A. Lombardo, R. V. Gorbachev, A. N. Grigorenko, A. K. Geim, A. C. Ferrari, and K. S. Novoselov, *Nature Commun.* **2**, 458 (2011).
- [4] A. H. Castro Neto, F. Guinea, N. M. R. Peres, K. S. Novoselov, and A. K. Geim, *Rev. Mod. Phys.* **81**, 109 (2009).
- [5] J. Yan, M.-H. Kim, J. A. Elle, A. B. Sushkov, G. S. Jenkins, H. M. Milchberg, M. S. Fuhrer, and H. D. Drew, *Nature Nanotech.* **7**, 472 (2012).
- [6] B. Huard, N. Stander, J. A. Sulpizio, and D. Goldhaber-Gordon, *Phys. Rev. B* **78**, 121402 (2008).
- [7] M. Freitag, T. Low, F. Xia, and P. Avouris, *Nature Photonics* **7**, 53 (2013).
- [8] N. M. Gabor, J. C. W. Song, Q. Ma, N. L. Nair, T. Taychatanapat, K. Watanabe, T. Taniguchi, L. S. Levitov, and P. Jarillo-Herrero, *Science* **334**, 648 (2011).
- [9] P. A. George, J. Strait, J. Dawlaty, S. Shivaraman, M. Chandrashekar, F. Rana, and M. G. Spencer, *Nano Lett.* **8**, 4248 (2008).
- [10] C. H. Lui, K. F. Mak, J. Shan, and T. F. Heinz, *Phys. Rev. Lett.* **105**, 127404 (2010).
- [11] W.-K. Tse, E. H. Hwang, and S. D. Sarma, *Appl. Phys. Lett.* **93**, 023128 (2008).
- [12] J.-H. Chen, C. Jang, S. Xiao, M. Ishigami, and M. S. Fuhrer, *Nature Nanotech.* **3**, 206 (2008).
- [13] R. Bistritzer and A. H. MacDonald, *Phys. Rev. Lett.* **102**, 206410 (2009).
- [14] J. K. Viljas and T. T. Heikkilä, *Phys. Rev. B* **81**, 245404 (2010).
- [15] J. H. Strait, H. Wang, S. Shivaraman, V. Shields, M. Spencer, and F. Rana, *Nano Lett.* **11**, 4902 (2011).
- [16] D. Sun, G. Aivazian, A. M. Jones, J. S. Ross, W. Yao, D. Cobden, and X. Xu, *Nature Nanotech.* **7**, 114 (2012).
- [17] T. Low, V. Perebeinos, R. Kim, M. Freitag, and P. Avouris, *Phys. Rev. B* **86**, 045413 (2012).
- [18] S. Winnerl, M. Orlita, P. Plochocka, P. Kossacki, M. Potemski, T. Winzer, E. Malic, A. Knorr, M. Sprinkle, C. Berger, W. A. de Heer, H. Schneider, and M. Helm, *Phys. Rev. Lett.* **107**, 237401 (2011).
- [19] S. Winnerl, F. Göttfert, M. Mittendorff, H. Schneider, M. Helm, T. Winzer, E. Malic, A. Knorr, M. Orlita, M. Potemski, M. Sprinkle, C. Berger, and W. A. de Heer, *J. Phys.: Condens. Matter* **25**, 054202 (2013).
- [20] M. W. Graham, S.-F. Shi, D. C. Ralph, J. Park, and P. L. McEuen, *Nature Phys. AOP* (2012), DOI:10.1038/nphys2493.
- [21] J. C. W. Song, M. S. Rudner, C. M. Marcus, and L. S. Levitov, *Nano Lett.* **11**, 4688 (2011).
- [22] J. Yan and M. S. Fuhrer, *Nano Lett.* **10**, 4521 (2010).
- [23] X. Xu, N. M. Gabor, J. S. Alden, A. M. van der Zande, and P. L. McEuen, *Nano Lett.* **10**, 562 (2010).
- [24] D. K. Efetov and P. Kim, *Phys. Rev. Lett.* **105**, 256805 (2010).
- [25] J. Yan, E. A. Henriksen, P. Kim, and A. Pinczuk, *Phys. Rev. Lett.* **101**, 136804 (2008).
- [26] J. Martin, N. Akerman, G. Ulbricht, T. Lohmann, J. H. Smet, K. von Klitzing, and A. Yacoby, *Nature Phys.* **4**, 144 (2008).
- [27] J. C. W. Song, M. Y. Reizer, and L. S. Levitov, *Phys. Rev. Lett.* **109**, 106602 (2012).
- [28] L. M. Zhang, Z. Q. Li, D. N. Basov, M. M. Fogler, Z. Hao, and M. C. Martin, *Phys. Rev. B* **78**, 235408 (2008).